

---

# Hat Basis Functions and Their Usage in Numerical Evaluation of Hankel Transforms

**Dr. Manoj Prakash Tripathi**

Department of Mathematics,  
Udai Pratap Autonomous College,  
Varanasi, India

---

## Abstract

This article deals with numerical evaluation of Hankel transform of order  $\nu > -1$  in which an algorithm is developed to compute it numerically. In the present article, we have developed the algorithm by approximating the rapidly oscillating component  $J_\nu(pr)$  in the expression for Hankel transform by hat basis functions. Hat basis functions are defined in the manuscript in their general form. We further give error analysis and corroborate our theoretical findings by various numerical illustrations.

## 1. Introduction

The general Hankel transform pair for Bessel function of order  $\nu$  is defined as [1, 2]

$$H_\nu[f(r); p] = \int_0^\infty r f(r) J_\nu(pr) dr = F_\nu(p)$$

(1.1)

Hankel Transform is self reciprocal; its inverse is given by

$$H_{\nu}^{-1} [F_{\nu}(p); r] = \int_0^{\infty} p F_{\nu}(p) J_{\nu}(pr) dp = f(r)$$

(1.2)

where  $J_{\nu}$  is the  $\nu$  th-order Bessel function of first kind.

Due to presence of rapidly oscillating component  $J_{\nu}(pr)$  in the integrand of Hankel transform, analytical evaluations of Hankel transforms (Eq.(1.1)) and its inverse (Eq.(1.2)) involve deep and rigorous mathematical analysis. The numerical computations of Hankel transform are difficult because of the oscillatory behaviour of the Bessel functions and infinite length of the interval involved in it. In the recent past we have seen that several quality research papers have been published in which numerical computations are elaborately described for computation of Hankel transform for both zero- order [3-10] and high – orders [11-19].

Some of the authors have used a simplistic way of separating the kernel in the integrand of Hankel transform as a product of two components. The first component is a slowly varying component while the second component is highly oscillating. In our case the slowly varying component is  $rf(r)$  where as rapidly oscillating component is  $J_{\nu}(pr)$ . Some of the approaches towards the evaluation of HT involve the approximation of slowly varying component  $rf(r)$  by means of different wavelets or approximating polynomials and very efficient algorithms have been proposed using the idea. But Singh et al. [16] first time proposed a new algorithm, by approximating the rapidly oscillating component  $J_{\nu}(pr)$  using Bernstein polynomials. The idea of numerical computation of HT by approximation of its rapidly oscillating component  $J_{\nu}(pr)$  motivated me for the

present work. In this article, hat basis functions are used to approximate this rapidly oscillating component which is an entirely different approach than other available methods, thereby getting an efficient and stable algorithm for the numerical evaluation of the HT of order  $\nu > -1$ .

## 2. Hat functions and their associated properties

Hat functions [19] are defined on the domain  $[0, 1]$ . These are continuous functions with shape of hats (Fig 2.1), when plotted on a two dimensional plane. The interval  $[0, 1]$  is divided into  $n$  subintervals  $[ih, (i + 1)h]$ ,  $i = 0, 1, 2, \dots, n - 1$ , of equal lengths  $h$  where  $h = 1/n$ . The hat function's family of first  $(n + 1)$  hat functions is defined as follows:

$$\psi_0(t) = \begin{cases} \frac{h-t}{h}, & 0 \leq t < h, \\ 0, & \text{otherwise,} \end{cases} \quad (2.1)$$

$$\psi_i(t) = \begin{cases} \frac{t-(i-1)h}{h}, & (i-1)h \leq t < ih, \\ \frac{(i+1)h-t}{h}, & ih \leq t < (i+1)h, \quad i = 1, 2, \dots, n-1, \\ 0, & \text{otherwise,} \end{cases} \quad (2.2)$$

$$\psi_n(t) = \begin{cases} \frac{t-(1-h)}{h}, & 1-h \leq t \leq 1, \\ 0, & \text{otherwise.} \end{cases} \quad (2.3)$$

From the definition of hat functions it is obvious that

$$\psi_i(kh) = \begin{cases} 1, & i = k, \\ 0, & i \neq k, \end{cases} \tag{2.4}$$

The hat functions  $\Psi_i(t)$  are continuous, linearly independent and are in  $L^2[0, 1]$ . Further a function  $L^2[0, 1]$  may be approximated as

$$f(t) \approx \sum_{i=0}^{i=n} f_i \Psi_i(t) = f_0 \Psi_0(t) + f_1 \Psi_1(t) + f_2 \Psi_2(t) + \dots + f_n \Psi_n(t) \tag{2.5}$$

The important aspect of using extended hat functions in the approximation of function  $f(t)$  lies in the fact that the coefficients  $f_i$  in the Eq. (2.5), are given by

$$f_i = f(ih), \quad \text{for } i = 0, 1, 2, 3, \dots, n \quad \text{where } h = 1/n \tag{2.6}$$

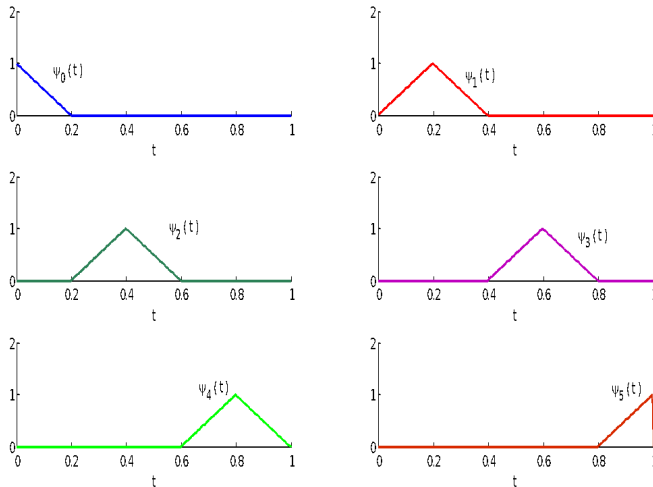


**Fig. 2.1.** The graph of six hat functions  $\Psi_0, \Psi_1, \Psi_2, \Psi_3, \Psi_4, \Psi_5$  for  $n = 5, h = 0.2$

**3. Algorithm**

In order to compute the HT  $\int_0^\infty rf(r) J_\nu(pr) dr$ , we divide the domain space  $(0, \infty)$  into two regions  $(0, R)$  and  $(R, \infty)$ . From physical point of view the input signal  $f(r)$  decays in the region  $(R, \infty)$  and vanishes in this domain. So, the Hankle transform

$$H_\nu[f(r); p] = \int_0^\infty rf(r) J_\nu(pr) dr = F_\nu(p) \text{ in Eq. (1.1) reduces into}$$

finite domain space form given by

$$\widehat{H}_\nu[f(r); p] = \int_0^R rf(r) J_\nu(pr) dr = \widehat{F}_\nu(p)$$

$$(3.1)$$

By scaling Eq. (3.1) may be written as

$$\widehat{F}_\nu(p) = \int_0^1 rf(r) J_\nu(pr) dr \tag{3.2}$$

which is known as the finite Hankel transform (FHT). Here we incorporate our approximation scheme on rapidly oscillating function  $J_\nu(pr)$  by using hat basis functions as given in Eqs.

(2.5) and (2.6), and we approximate it as

$$\begin{aligned} J_\nu(pr) &\approx J_\nu(0)\Psi_0(r) + J_\nu(ph)\Psi_1(r) + J_\nu(2ph)\Psi_2(r) + \dots + J_\nu(nph)\Psi_n(r) \\ &= \sum_{i=0}^{i=n} J_\nu(iph)\Psi_i(r) . \end{aligned} \tag{3.3}$$

Using the approximation in (3.3), Eq. (3.2) may be written as

$$\widehat{F}_\nu(p) \approx \int_0^1 rf(r) \sum_{i=0}^{i=n} J_\nu(iph)\Psi_i(r) dr = \sum_{i=0}^{i=n} J_\nu(iph) \int_0^1 rf(r) \Psi_i(r) dr$$

(3.4)

The expression in the Equation (3.4) involves integral  $\int_0^1 r f(r) \Psi_i(r) dr$  which may be easily calculated because  $f(r)$  is known function and  $\Psi_i(r)$  is a linear polynomial  $\forall i$ .

**4. Error Analysis**

In this section we present error estimation, involved in the computations of  $J_v(pr)$  and hence in FHT  $\widehat{F}_v(p)$  when  $J_v(pr)$  is approximated via hat basis functions. For  $p \in [0, P]$ , from Eq. (3.3) we have

$$J_v(pr) \simeq \sum_{i=0}^{i=n} J_v(ip h) \Psi_i(r) \tag{4.1}$$

Let the R.H.S. of Eq. (4.1) is denoted by  $\bar{J}_v(pr)$  i.e.

$$\bar{J}_v(pr) = \sum_{i=0}^{i=n} J_v(ip h) \Psi_i(r) \tag{4.2}$$

From equation (4.2) and Eq.(2.4), the value of  $\bar{J}_v(pr)$  at  $j^{\text{th}}$  nodal point  $r = jh, j = 0, 1, 2, \dots, n$  is given by

$$\begin{aligned} \bar{J}_v(pjh) &= \sum_{i=0}^{i=n} J_v(ip h) \Psi_i(jh) \\ &= J_v(jph) \Psi_j(jh) + J_v(jph + ph) \Psi_{j+1}(jh) = J_v(jph). \end{aligned}$$

Thus the approximation  $\bar{J}_v(pr)$  gives exact value of  $J_v(pr)$  at all nodal points  $r = jh, j = 0, 1, \dots, n$ .

Further if  $r$  lies between two consecutive integer multiples of  $h$  i.e.  $jh < r < (j + 1)h, j = 0, 1, \dots, nr$ , then from Eqs.(4.2), we have

$$\begin{aligned} \bar{J}_v(pr) &= J_v(jph)\Psi_j(r) + J_v((j + 1)ph)\Psi_{j+1}(r) \\ &= J_v(jph)\left[\frac{(j+1)h-r}{h}\right] + J_v(jph + ph)\left[\frac{r-jh}{h}\right] \\ &\hspace{15em} \text{(Using (2.3-2.4))} \\ &= J_v(jph) - jph\left[\frac{J_v(jph+ph)-J_v(jph)}{ph}\right] + rp\left[\frac{J_v(jph+ph)-J_v(jph)}{ph}\right]. \end{aligned} \tag{4.3}$$

As  $h \rightarrow 0$ , the expression in R.H.S. of Eq.(4.3) may be written as

$$\bar{J}_v(pr) \simeq J_v(jph) - jphJ'_v(jph) + prJ'_v(jph) \tag{4.4}$$

By expanding  $J_v(pr)$  in form of Taylor's series in the powers of  $(pr - jph)$ , we have

$$J_v(pr) = \sum_{k=0}^{\infty} \frac{(pr-jph)^k}{k!} J_v^{(k)}(jph), \tag{4.5}$$

where  $J_v^{(k)}$  denotes the  $k^{th}$  order derivative of  $J_v$ .

Using Eqs.(4.4) and (4.5), the error between exact and approximate values of  $J_v(pr)$  is given by

$$\begin{aligned} J_v(pr) - \bar{J}_v(pr) &= \sum_{k=2}^{\infty} \frac{(pr-jph)^k}{k!} J_v^{(k)}(jph) \\ &= \frac{(pr-jph)^k}{2!} J_v^{(2)}(jph) + O(pr - pjh)^3 \end{aligned} \tag{4.6}$$

Since  $pjh < pr < p(j + 1)h$  so  $(pr - pjh) < ph$ . Replacing  $h$  by  $1/n$  and using Eq.(4.6), we have

$$J_v(pr) - \bar{J}_v(pr) \leq \frac{p^2}{2n^2} J_v''(jph) + O\left(\frac{p^3}{n^3}\right) \tag{4.7}$$

Thus

$$\left| J_v(pr) - \bar{J}_v(pr) \right| \leq \frac{p^2}{2n^2} \left| J_v''(jph) \right| + O\left(\frac{p^3}{n^3}\right) \tag{4.8}$$

As we know that

$$J_v'(x) = \frac{1}{2} [J_{v-1}(x) - J_{v+1}(x)]$$

so for a constant  $\lambda$ , we have

$$J'_v(\lambda x) = \frac{\lambda}{2} [J_{v-1}(\lambda x) - J_{v+1}(\lambda x)]$$

and thus

$$J''_v(\lambda x) = \frac{\lambda^2}{4} [J_{v-2}(\lambda x) - 2J_v(\lambda x) + J_{v+2}(\lambda x)] \tag{4.9}$$

Using Eq. (4.9) in (4.8), for  $\lambda = jh$ , Eq (4.8) may be rewritten as

$$\begin{aligned} |J_v(pr) - \bar{J}_v(pr)| &\leq \frac{j^2 h^2 p^2}{8n^2} |J_{v-2}(pjh) - 2J_v(jph) + J_{v+2}(jph)| \\ &\quad + O\left(\frac{p^3}{n^3}\right) \end{aligned} \tag{4.10}$$

Since  $J_v(pjh) \leq 1$ , so from Eq. (4.10), we get

$$|J_v(pr) - \bar{J}_v(pr)| \leq \frac{j^2 h^2 p^2}{2n^2} + O\left(\frac{p^3}{n^3}\right). \tag{4.11}$$

If we denote the approximate finite Hankel transform of  $f(r)$  by

$$\widehat{F}(r) \text{ i.e. } \widehat{F}(r) = \int_0^1 r f(r) \bar{J}_v(pr) dr$$

, then Eq.(4.11) is used to obtain the absolute error  $\varepsilon_n(p)$  between exact FHT  $\widehat{F}(r)$  and

approximate FHT  $\widehat{F}(r)$ , as follows:

$$\begin{aligned} \varepsilon_n(p) &= \left| \widehat{F}(r) - \widehat{F}(r) \right| = \left| \int_0^1 r f(r) (J_v(pr) - \bar{J}_v(pr)) dr \right| \\ &= \left| \sum_{j=0}^{n-1} \int_{jh}^{(j+1)h} r f(r) (J_v(pr) - \bar{J}_v(pr)) dr \right| \\ &\leq \sum_{j=0}^{n-1} \int_{jh}^{(j+1)h} r |f(r)| |J_v(pr) - \bar{J}_v(pr)| dr \\ &\leq \sum_{j=0}^{n-1} \left[ \frac{j^2 h^2 p^2}{2n^2} + O\left(\frac{p^3}{n^3}\right) \right] \int_{jh}^{(j+1)h} r |f(r)| dr \end{aligned} \tag{4.12}$$



(Using Eq.(4.11))

In all the numerical illustrations  $|f(r)| \leq 1$  thus from (4.12)

$$\begin{aligned}
 \varepsilon_n(p) &\leq \sum_{j=0}^{n-1} \left[ \frac{j^2 h^2 p^2}{2n^2} + O\left(\frac{p^3}{n^3}\right) \right] \int_{jh}^{(j+1)h} r \, dr \\
 &= \sum_{j=0}^{n-1} \left[ \frac{j^2 p^2}{2n^4} + O\left(\frac{p^3}{n^3}\right) \right] \left(j + \frac{1}{2}\right) h^2 \\
 &= \sum_{j=0}^{n-1} \left[ \frac{j^2 \left(j + \frac{1}{2}\right) p^2}{2n^6} \right] + \sum_{j=0}^{n-1} O\left(\frac{p^3}{n^3}\right) \left(j + \frac{1}{2}\right) h^2 \\
 &= \sum_{j=0}^{n-1} \left[ \frac{j^2 \left(j + \frac{1}{2}\right) p^2}{2n^6} \right] + O\left(\frac{p^3}{n^3}\right) h^2 \sum_{j=0}^{n-1} \left(j + \frac{1}{2}\right) \\
 &= \frac{p^2}{2n^6} \sum_{j=0}^{n-1} j^2 \left(j + \frac{1}{2}\right) + O\left(\frac{p^3}{n^3}\right) \\
 &= \frac{(1-1/n)[3-(1/n)-(1/n^2)]p^2}{24n^2} + O\left(\frac{p^3}{n^3}\right) \tag{4.13}
 \end{aligned}$$

Thus we may state the following theorem:

**Theorem:** For input signal  $f(r)$  with absolute value lying in  $(0, 1]$ , the absolute error  $\varepsilon_n(p)$  between exact FHT  $\widehat{F}(r)$  and approximate FHT  $\widehat{\widehat{F}}(r)$  is of order  $O\left(\frac{p^3}{n^3}\right)$  where the symbols used are as above.

**5. Numerical Illustrations:**

The test problems included in this manuscript are solved with and without random perturbations (noises) to illustrate the efficiency and stability of the proposed algorithm. The graphs are sketched for different values of step sizes. The terms  $E_0(p)$ ,  $E_1(p)$

and  $E_2(p)$  and denote errors between exact and approximate HT with noise terms  $\alpha_0, \alpha_1$  and  $\alpha_2$  respectively. In the text boxes of the figures  $E_0(p), E_1(p)$  and  $E_2(p)$  have been denoted by  $E0(p), E1(p)$  and  $E2(p)$  respectively. The parameter  $p$  ranges between 0 to 30.

**Example 1:** A very important, and often used function, is the Circ function that can be defined piecewise as

$$Circ(r/a) = 0 \text{ or } 1 \quad \text{according as } r \leq a \quad \text{or } r > a \quad (5.1)$$

respectively.

The zeroth-order HT of  $Circ(r/a)$  is the Sombrero function [16], that will be written as  $S_0(p)$  with the following analytical

$$\text{expression } S_0(p) = a^2 \frac{J_1(ap)}{ap} .$$

Eq. (3.4) is used to obtain the finite HT  $\widehat{F}_0(p)$  of  $Circ(r/a)$ , for  $a = 1$ , as follows:

$$\widehat{F}_0(p) \simeq \int_0^1 r \text{Circ}(r) \sum_{i=0}^n J_0(pih) \Psi_i(r) dr = \sum_{i=0}^n J_0(pih) \int_0^1 r \Psi_i(r) dr \quad (5.2)$$

Using Eqs.(2.1-2.3), Eq. (5.2) becomes

$$\widehat{F}_0(p) \simeq J_0(0) \int_0^h r \frac{h-r}{h} dr + \sum_{i=0}^n J_0(pih) \left[ \int_{(i-1)h}^{ih} r \left( \frac{r-(i-1)h}{h} \right) dr + \int_{ih}^{(i+1)h} r \left( \frac{(i+1)h-r}{h} \right) dr \right]$$

$$+ J_0(p) \int_{1-h}^1 r \left( \frac{r-(i-1)h}{h} \right) dr. \tag{5.3}$$

The integrals involved in Eq. (5.3) are easily calculated and the value of  $\widehat{F}_0(p)$  can be obtained for different  $p$ . The exact Hankel transforms and approximate Hankel transforms of  $Circ(r)$  function are denoted by  $S_0(p)$  and  $H_0(p)$  respectively. In the text box of Fig.5.1, exact and approximate zeroth-order Hankel transforms have been represented by  $S0(p)$  and  $H0(p)$  respectively. In Fig. 5.2, the error between exact HT and approximate HT (with zero noise) is shown for  $n = 10000$ . The maximum error is of order  $10^{-9}$ . The graph in this figure also justifies the error analysis done in Section - 4 which characterises the increasing nature of the error with  $p$ . Fig. 5.3 compares the different errors (with and without perturbations) in calculating finite HT.

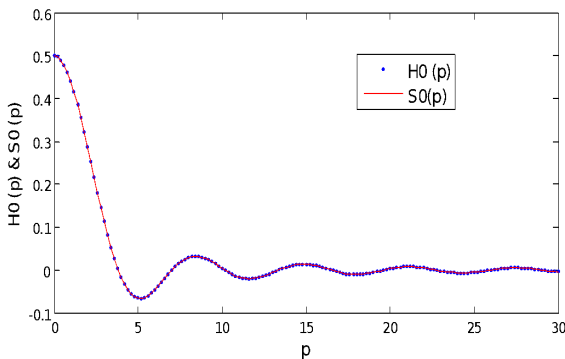


**Fig5.1.** Exact HT  $S_0(p)$  and approximate HT  $H_0(p)$  for  $n = 100$  in

Ex. 1

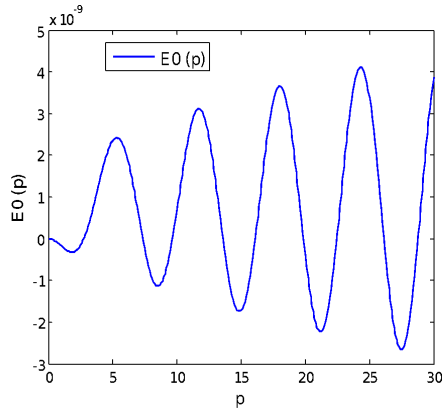


**Fig5.2.** Error  $E_0(p)$  with zero noise for  $n = 10000$  in Ex1.

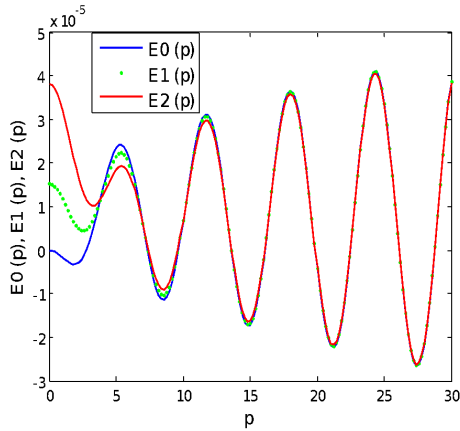


**Fig 5.3.**  $E_0(p), E_1(p), E_2(p)$  for  $n = 100$  in Ex. 1

**Example 2.** Consider the function  $f(r) = \sqrt{(1 - r^2)}$ ,  $0 \leq r \leq 1$  given in [17], for which

$$F_1(p) = \begin{cases} \pi \frac{J_1^2(p/2)}{2p}, & 0 < p < \infty, \\ 0, & p = 0. \end{cases} \tag{6.4}$$

Numerical evaluation of  $F_1(p)$  has been achieved by Baraket et al. [11], by using Filon quadrature philosophy but again the associated error is appreciable for  $p < 1$ . The exact HT for the example is  $F_1(p)$  and approximate HT is denoted by  $H_1(p)$ . Fig. 5.4 shows the comparison between exact and approximate Hankel transform in which  $F_1(p)$  and  $H_1(p)$  have been denoted by  $F1(p)$  and  $H1(p)$  respectively. Fig. 5.5 depicts the graph of error  $E_0(p)$  for  $n = 10000$ . In Fig. 7, the errors  $E_0(p)$ ,  $E_1(p)$ ,  $E_2(p)$  for  $n = 100$  are plotted.

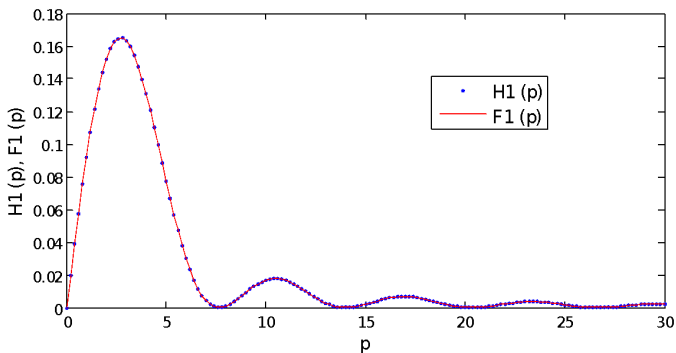


**Fig 5.4.** Comparison between  $H_1(p)$  and  $F_1(p)$  for  $n = 100$ , Ex.2

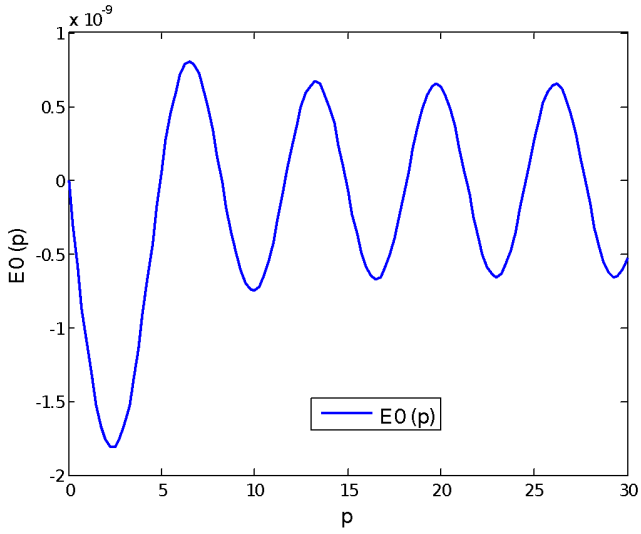


**Fig 5.6.** Error  $E_0(p)$  for  $n = 10000$  in Ex. 2

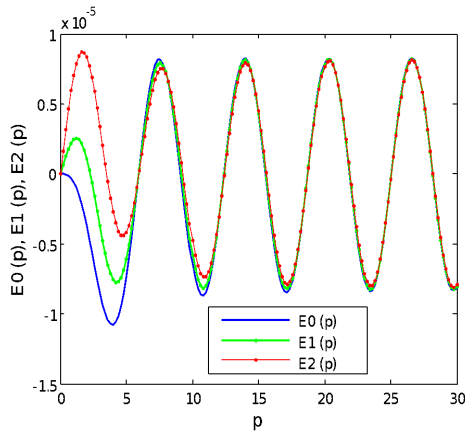


**Fig 5.7.**  $E_0(p)$ ,  $E_1(p)$ ,  $E_2(p)$ , for  $n = 10000$  in Ex. 2

**Example 3.** Let  $f(r) = r^\nu \sin\left(\frac{\pi r^2}{4}\right)$ ,  $0 \leq r < 1$ , then

$$F_\nu(p) = \frac{1}{\sqrt{2}} \left(\frac{\pi}{2}\right)^{-\nu-1} p^\nu \left[ U_{\nu+1}\left(\frac{\pi}{2}, p\right) - U_{\nu+2}\left(\frac{\pi}{2}, p\right) \right] \tag{6.7}$$

(obtained from [16, p.34, Eq.(16)] by putting  $a = \pi/4$ ,  $b = 1$ ), where  $U_\nu(w, p)$  is a Lommel's function [16] of two variables, given by

$$U_\nu(w, p) = \frac{1}{2\sqrt{p}} \left[ \sum_{r=0}^M (-1)^r \left(\frac{\pi}{2p}\right)^{2r} \right] \left( J_{\nu+2r+1}(p) - \left(\frac{\pi}{2p}\right) J_{\nu+2r+2}(p) \right)$$

as  $M \rightarrow \infty$ .

We take  $\nu = 3/2$  and show comparison between exact HT  $F_{3/2}(p)$  and approximate HT  $H_{3/2}(p)$  in Fig. 5.8. Fig. 5.9 shows the error  $E_0(p)$  with zero noise for  $n = 10000$ .

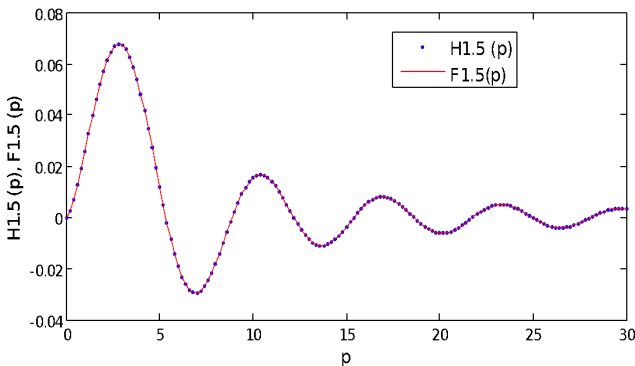


**Fig 5.8.**  $F_{3/2}(p)$ ,  $H_{3/2}(p)$  for  $n = 100$  in Ex. 3

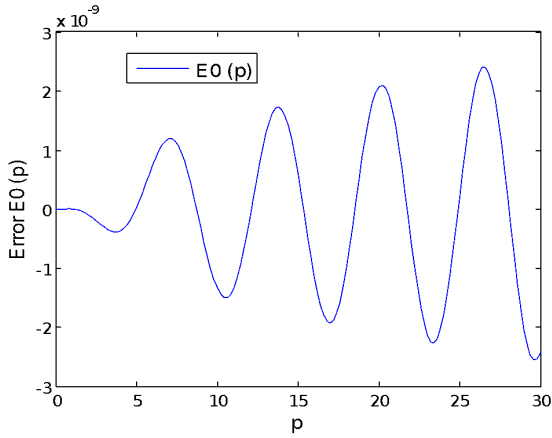


Fig 5.9. Error  $E_0(p)$  with zero noise for  $n = 10000$  (Ex.3)

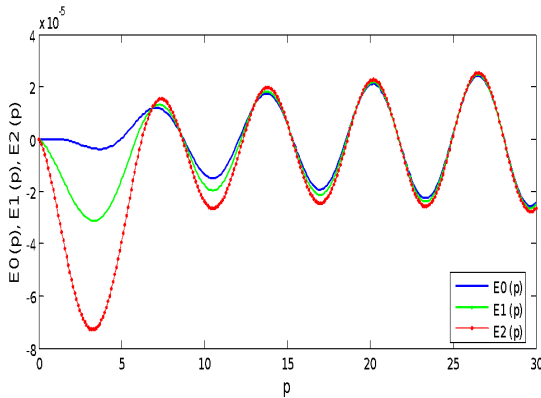


Fig. 17.  $E_0(p), E_1(p), E_2(p)$ , for  $n = 100$  in Ex. 3

### Conclusions



In the present manuscript, the application and scope of Hat functions have been extended to develop an efficient algorithm for numerical evaluation of finite Hankel transform, together with error analysis. The response shown by the algorithm is very satisfactory. The results are matched with some known problems with better accuracy.

### References

1. *Sneddon, I.N.: The use of Integral Transforms. McGraw-Hill (1972).*
2. *R. Bracewell, The Fourier transform and its application (McGraw-Hill, New York, 1965).*
3. *Magni, V., Cerullo, G., Silvestri, D.: High-accuracy fast Hankel transform for optical beam Propagation. J. Opt. Soc. Am. A 12, 2031-2033 (1992).*
4. *Barakat, R., Parshall, E., Sandler, B.H.: Zero-order Hankel transform algorithms based on Filon quadrature philosophy for diffraction optics and beam propagation. J. Opt. Soc. Am. A 15, 652-659 (1998).*
5. *Mook, D.R.: An algorithm for numerical evaluation of Hankel and Abel transform. IEEE Trans. Acoust. Speech Signal Process ASSP-31, 979-985 (1983).*
6. *Hansen, E.V.: Fast Hankel transform algorithms. IEEE Trans. Acoust. Speech Signal Process ASSP-33, 666-671 (1985).*
7. *Suter, B.W.: Fast nth order Hankel transform algorithm. IEEE Trans. Signal Process 39,532-536 (1991).*

8. Hansen, E.V.: Correction to Fast Hankel transform algorithms. *IEEE Trans. Acoust. Speech Signal Process ASSP-34*, 623-624 (1986).
9. Kanghe Xie, Yulin Wang, Kun Wang, Xin Cai, Application of Hankel transform to boundary value problems of water flow due to circular source, *Applied Mathematics and Computation*, 216(2010) 1469-1477.
10. Ferrari, J.A.: Fast Hankel transform of order zero. *J. Opt. Soc. Am. A 12*, 1812-1813 (1995).
11. Barakat, R., Parshall, E.: Numerical evaluation of the zero-order Hankel transform using Filon quadrature philosophy. *Appl. Math. Lett 9 (5)*, 21-26 (1996).
12. Suter, B.W.: Fast  $n$ th order Hankel transform algorithm. *IEEE Trans. Signal Process 39*, 532-536 (1991).
13. Markham, J., Conchello, J.A.: Numerical evaluation of Hankel transform for oscillating Function. *J. Opt. Soc. Am. A 20*, 621-630 (2003).
14. Postnikov, E.B.: About calculation of the Hankel transform using preliminary wavelet transform. *J. Applied Maths 6*, 319-325 (2003).
15. Singh, V.K., Singh, O.P., Pandey, R.K.: Numerical evaluation of Hankel transform by using linear Legendre multiwavelets. *Compu. Phys. Commun 179*, 424-429 (2008).
16. Singh, V.K., Singh, O.P., Pandey, R.K.: Efficient algorithms to compute Hankel transforms using Wavelets. *Compu. Phys. Commun, 179*, 812-818 (2008).
17. Rajesh K. Pandey, Om P. Singh, Vineet K. Singh, A stable algorithm for numerical evaluation of Hankel Transforms using Haar wavelets, *Numerical algor(2010)53:451-466*

18. Om P. Singh, Vineet K. Singh, Rajesh K. Pandey, *An efficient and stable algorithm for numerical evaluation of Hankel Transforms*, *J. Appl. Maths. & Informatics*, No. 5- 6, pp.1055-1071
19. Manoj P. Tripathi, B.P.Singh, Om P .Singh, *Stable Numerical Evaluation of Finite Hankel Transforms and Their Application*; *International Journal of Analysis Volume 2014*, Article ID 670562, <http://dx.doi.org/10.1155/2014/670562>